ISSN 1392–1320 MATERIALS SCIENCE (MEDŽIAGOTYRA). Vol. 17, No. 2. 2011

On the Properties of Yttria-Stabilized Zirconia Thin Films Prepared by Sol-Gel Method

Artūras ŽALGA [1], Brigita ABAKEVIČIENĖ [2], Aleksej ŽARKOV [1], Aldona BEGANSKIENĖ [1], Aivaras KAREIVA [1], Sigitas TAMULEVIČIUS [2] *

[1] *Faculty of Chemistry, Vilnius University, Naugarduko 24, LT-03225 Vilnius, Lithuania*
[2] *Institute of Materials Science of Kaunas University of Technology, Savanoriu av. 271, LT-50131 Kaunas, Lithuania*

Received 22 March 2011; accepted 02 May 2011

The synthesis of nanostructured films of 20 mol% Y_2O_3 stabilized ZrO_2 on corundum (Al_2O_3) substrates was performed from different sols using dip-coating technique. All obtained samples were repeatedly annealed at 800 °C temperature after each dipping procedure and fully characterized by X-ray diffraction (XRD) analysis. XRD data exhibited that at 800 °C temperature nano-sized $Y_{0.2}Zr_{0.8}O_2$ thin films with cubic (Fm-3m) crystal structure have been formed. The morphological features of obtained coatings were investigated by scanning electron microscopy (SEM) and atomic force microscopy (AFM). The surface tension and hydrophility of the synthesized films were determined by contact angle measurements (CAM).
Keywords: YSZ, sol-gel, suspensions, nanocoatings, solid oxide fuel cells.

1. INTRODUCTION

The system Y_2O_3-ZrO_2 has been extensively studied for last 50 years [1 – 3]. Although many metal-oxide and rare-earth oxide compositions have been examined as ionic conductors, zirconia-based materials are still the most common solid state electrolytes [4]. Yttria-doped zirconia materials due to their high ionic conductivity are used as electrolytes for electrode supported solid oxide fuel cells (SOFCs) [5]. The negligible electronic conductivity even under reducing atmosphere, the electrochemical stability as well as the mechanical properties of yttria stabilized zirconia (YSZ) facilitate the use in fuel-cell applications [5 – 7]. SOFCs are devices aimed at converting the chemical energy of a fuel directly into electricity [7]. A thin film concept for electrode supported designs based on the well-known YSZ is very promising, even though it has a lower ionic conductivity than other new materials [8]. However, the commercialization of SOFC on a big scale until today [9] does not occur.

The use of nanostructured ionic and mixed ionic-electronic conducting materials within fuel cells may facilitate lower operating temperatures and thus enhanced long-term stability of the cells [10 – 13]. For the development of SOFC systems in the intermediate-temperature regime of 500 °C < T < 750 °C, the nanoscaled thin films are of substantial interest. The decrease in physical dimensions down to the nanometer scale is often linked with a dramatic change of the physical and electrochemical properties of materials [14]. Although several techniques, including electrochemical vapour deposition, have been used to form thin films, it is desirable to develop cost-effective processes for broad commercial application of SOFCs [2, 3, 15, 16].

The technological applications of the sol-gel technique range in a very wide field, because of the versatility and simplicity of the method [17 – 24]. Compared to other techniques the sol-gel method has the advantages of a good control of the processing parameters. The use of sol-gel processing can eliminate major problems such as long diffusion paths, impurities and agglomeration, which will result in products with improved homogeneity [25 – 29]. The sol-gel process is based on liquid-phase hydrolysis of organo-metallic salts like metal alkoxides to form a colloidal sol and a condensation step with organic monomers to form a gel. To produce YSZ thin films different precursors have been reported: alkoxide precursors (zirconium and yttrium iso-propoxide, zirconium *n*-propoxide and yttrium propoxide), halogenide precursors (zirconium oxychloride and yttrium nitrate), nitrate and acetate precursors [30].

In this paper we report on the synthesis and characterization of YSZ thin films on the corundum substrates using dip-coating technique. During the dip-coating process the substrate is immersed in the precursor solution then withdrawn from the liquid [30]. For the preparation of stable sols two novel sol-gel synthesis approaches were suggested. Firstly, an aqueous sol-gel synthesis route was developed in which tartaric acid as a complexing agent has been used. While the second synthesis route was focused on the dissolution of the simple salts in the 1.2-propanediol, which was used as both solvent and complexing agent.

2. EXPERIMENTAL

In the first sol-gel synthesis approach (I) the Y-Zr-O nitrate-tartrate sol was prepared by an aqueous sol-gel synthesis route. In this case the 0.0025 mol of zirconium oxonitrate dihydrate ($ZrO(NO_3)_2 \cdot 2H_2O$, 99.9 %) was first dissolved in concentrated nitric acid solution (65 % HNO_3) by stirring at 70 °C – 80 °C. Secondly, tartaric acid (TA) with a molar ratio of Zr / TA = 0.25, dissolved in a small amount of distilled water was added with a continuous stirring at the same temperature. Next, after 5 h the

*Corresponding author. Tel.: +370-37-313432; fax.: +370-37-313432.
E-mail address: *sigitas.tamulevicius@ktu.lt* (S. Tamulevičius)

stoichiometric amount (0.000555556 mol) of yttrium nitrate hexahydrate ($Y(NO_3)_3 \cdot 6H_2O$, 99.99 %) dissolved in distilled water was mixed with the previous solution. Finally, the same amount of the aqueous solution of the complexing agent TA was repeatedly added to the reaction mixture to prevent crystallization of metal salts during the gelation process. The beaker with the solution was closed with a watch glass and left for 1 h with continuous stirring. The obtained clear solution was concentrated by slow evaporation at 80 °C in an open beaker. A pale yellow transparent Y-Zr-O nitrate-tartrate sol formed after nearly 60 % of the water has been evaporated under continuous stirring.

In the second sol-gel synthesis approach (II) the Y-Zr-O nitrate sol in 1.2-propanediol was prepared. Firstly, 0.0025 mol (90 %) of $ZrO(NO_3)_2 \cdot 2H_2O$ was dissolved in 50 ml of 1.2-propanediol at 60 °C – 75 °C under continuous stirring. Next, 0.000555556 mol (10 %) of $Y(NO_3)_3 \cdot H_2O$ was added to the above solution. The beaker with the solution was closed with a watch glass and left for 1 h with continuous stirring at 90 °C – 95 °C temperature. Finally, a yellow transparent Y-Zr-O nitrate-1.2-propanediolate sol formed after all experimental procedures.

YSZ thin films were deposited onto commercial corundum (1.5 × 1.5) cm substrates (Al_2O_3) by dip-coating technique from the Y-Zr-O nitrate sols stabilized with tartaric acid or 1.2-propanediol, respectively. The films on corundum substrate were deposited at 5 mm/min immersion rate and were dried at room temperature for 24 h in air at ambient pressure in a horizontal position. Afterwards, the dried coated substrate was annealed at 800 °C temperature in air for 1 h. According to [31] at this temperature the crystallization process begins and presence of a pure cubic phase of yttria-stabilized zirconia was reported for the YSZ sol-gel film. This process in our case was repeated to build up the desired film thickness that varied between 400 nm and 1 μm and was dependent on dipping counts during the synthesis route (Fig. 1).

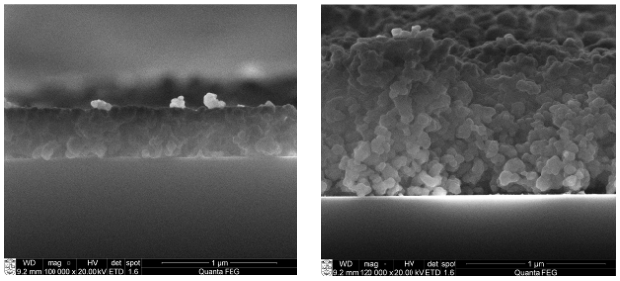

a b

Fig. 1. SEM micrographs of cross-sections of YSZ thin films: (a) after 2 dipping counts and 2 annealing procedures prepared by synthesis route (II), (b) after 30 dipping counts and 30 annealing procedures prepared by synthesis route (II)

X-ray diffraction analysis (XRD) was performed on a Bruker AXE D8 Focus diffractometer with a LynxEye detector using Cu K_α radiation. The measurements were recorded at the standard rate of 1.5 2θ / min. The scanning electron microscope (SEM) QUANTA 200 FEI and atomic force microscope (AFM) NT-206 were used to study the surface morphology and microstructure of the obtained thin films. For the characterization of coating surface hydrophobicity, the measurements of a contact angle on KVS Instrument CAM 100 were performed. The instrument includes a CCD camera, a frame grabber, an adjustable sample stage and LAD light source. A micro-droplet of water (volume 6 μl) was allowed to fall onto the sample from a syringe tip to produce a sessile drop. Each image was analyzed with respect to base, height, and shape of the droplet, and from these values the contact angle (KVS instrument software) was measured on three different points of each sample, repeating the measurements at least twice. The KSV D™ dip-coating apparatus, KSV Instruments Ltd., was used for coating preparation. The standard immersing (5 mm/min) and withdrawal rates (20 mm/min) for dip-coating process were applied for all the samples. The obtained suspensions were sonificated for 30 min with a Sonic Vibracell ultrasonic reactor with a 2 mm-diameter titanium probe operating at 20 kHz.

3. RESULTS AND DISCUSSIONS

It is worth to note that XRD patterns of the YSZ films obtained from aqueous and non-aqueous sols (synthesis routes (I) and (II)) are very similar. Therefore, Fig. 2 represents the XRD pattern of YSZ films obtained from Zr-Y-O nitrate-1.2-propanediolate sol using dip-coating technique.

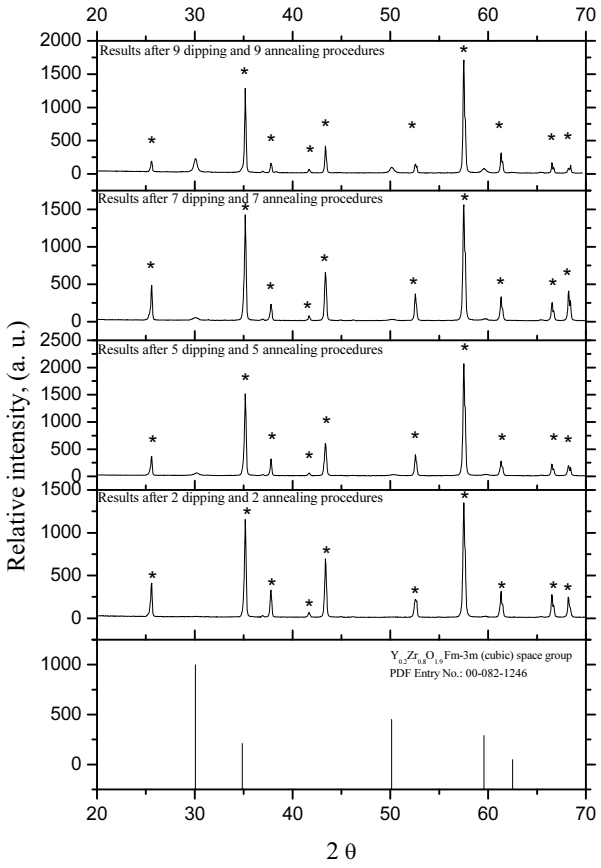

Fig. 2. XRD patterns of the YSZ samples annealed at 800 °C after each dipping procedure for 1 h in air (synthesis route (II)). * – characteristic peaks of the substrate (Al_2O_3), (the last inset shows intensity distribution for $Y_{0.2}Zr_{0.8}O_{1.9}$ for Fm-3m space group)

Moreover, these results present the influence of the number of coating procedures on the crystallization of YSZ coatings.

As seen from Fig. 2, even after seven immersing, withdrawals and annealing procedures no significant peaks attributable to the YSZ crystal phase are observed. However, already after nine dipping and annealing times the main four characteristic peaks attributable to the cubic YSZ crystal phase appear in the XRD pattern.

The XRD patterns of YSZ films obtained from YSZ suspension in 1.2-propanediol (synthesis route (II)) are shown in Fig. 3. As seen from Fig. 3, the same characteristic peaks of the YSZ phase could be distinguished in the XRD patterns even after 9 dipping and annealing procedures. Thus, according to the XRD analysis data all two suggested synthesis routes are suitable for the preparation of thin YSZ films on Al_2O_3 substrate.

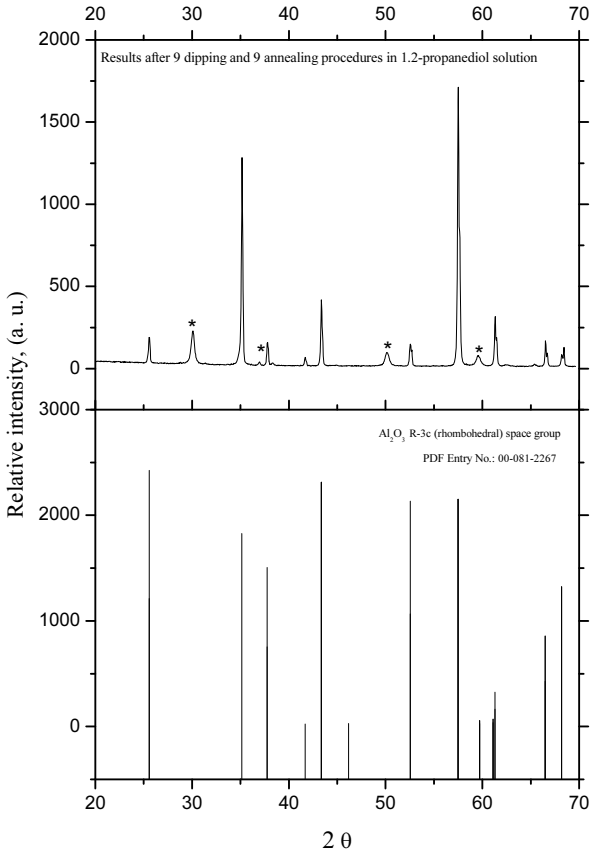

Fig. 3. XRD patterns of the YSZ samples annealed at 800 °C after each dipping procedure for 1 h in air (synthesis route (II)). * – characteristic peaks of the $Y_{0.2}Zr_{0.8}O_{1.9}$ cubic (Fm-3m) phase (the last inset shows intensity distribution for $Y_{0.2}Zr_{0.8}O_{1.9}$ for Fm-3m space group)

The surface morphology of obtained YSZ thin films by different synthesis routes was investigated by scanning electron microscopy. The representative SEM micrographs of YSZ thin film prepared by synthesis (I) and (II) approaches are shown in Fig. 4.

For better understanding of the crystal growth process of the YSZ layers and quantitative description of the surface morphology, we have investigated the influence of the number of dipping and annealing procedures on the morphology of the end products using atomic force microscopy. The AFM micrographs of corundum Al_2O_3 substrate and YSZ thin films obtained after 5 dipping and annealing procedures and prepared by the synthesis routes (I) and (II) are shown in Figs. 5, 6 (a) and (b), respectively.

Moreover, the SEM micrographs showed that almost identical features were observed for all the samples. Consequently, these results let us to conclude that surface microstructure of YSZ thin films are independent on the used synthesis route.

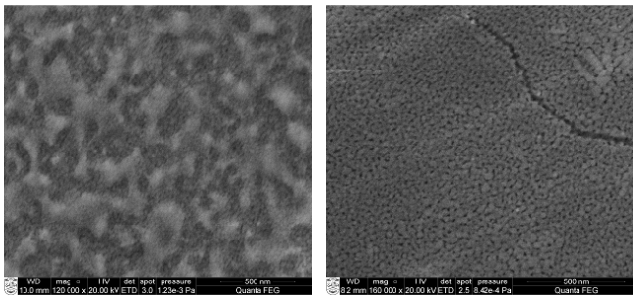

a b

Fig. 4. SEM micrographs of YSZ thin films after different dipping counts and annealing procedures and prepared by the different synthesis route: (a) 7 dipping by the synthesis route (I), (b) 7 dipping by the synthesis route (II)

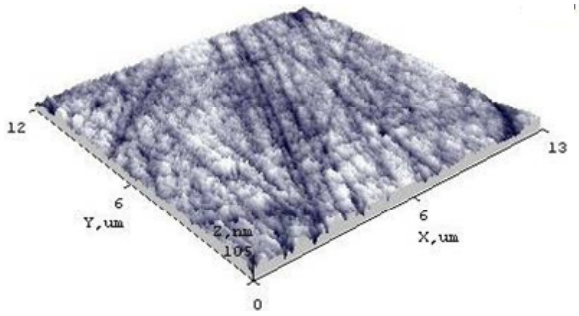

Fig. 5. AFM surface image of substrate (Al_2O_3, corundum)

Evidently, the AFM images of the samples obtained after 5 dipping and 5 annealing procedures in both (I and II) synthesis routes are very similar indicating that the root-mean-square (RMS) average roughness of 5 dipping of YSZ films is rather low (R_q varies between 8.3 nm and 7.8 nm) and is lower than the RMS average roughness (9.2 nm) of the alumina substrate (see Table 1).

The situation, however, significantly differs after longer dipping and annealing procedures. The AFM image of YSZ thin films obtained after 7 dipping and annealing procedures using aqueous synthesis route (I) is shown in Fig. 6 (c). The formation of spherical YSZ particles on the corundum substrate could be easily seen. The average of maximum height of particle size ranges between 52 nm and 122 nm. The AFM image of YSZ thin films obtained after seven dipping and annealing procedures using non-aqueous synthesis route (II) is shown in Fig. 6 (d).

However, during synthesis route (I) the YSZ particles on the surface are distributed more evenly.

Besides, the thickness of the YSZ films as well as roughness increases with increasing the dipping and annealing time (Fig. 1).

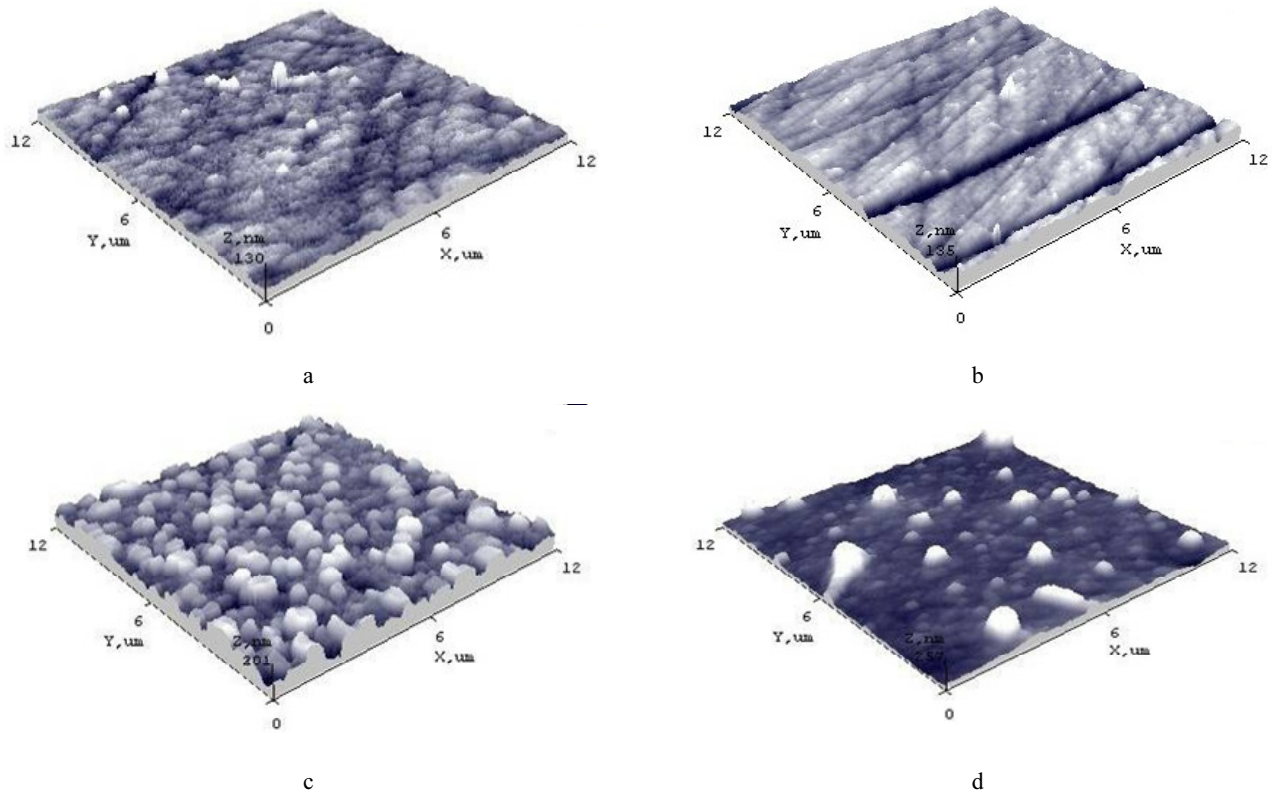

Fig. 6. AFM surface images of YSZ thin film obtained: (a) after 5 dipping and annealing procedures and prepared by the synthesis route (I), (b) after 5 dipping and annealing procedures and prepared by the synthesis route (II), (c) after 7 dipping and annealing procedures and prepared by the synthesis route (I), (d) after 7 dipping and annealing procedures and prepared by the synthesis route (II)

Table 1. AFM and contact angle measurements of YSZ coatings

Structure	Max. height, Z, nm	Average of max. height, Z_{mean}, nm	Root-mean-square average roughness, R_q, nm	Skewness, R_{sk}, nm
Al_2O_3 substrate	105.0	49.6	9.2	–0.3
5 dipping, synthesis route (I)	129.8	38.4	8.3	1.3
5 dipping, synthesis route (II)	135.3	52.7	7.8	-0.6
7 dipping, synthesis route (I)	256.9	121.5	26.9	0.3
7 dipping, synthesis route (II)	200.7	52.0	31.5	3.4

These facts illustrate that two proposed methods of YSZ synthesis allow formation of submicronic based materials (particle size varied between 80 nm and 180 nm) with a controlled morphology and mixing of species on the atomic scale like it was shown in [32]. These results are in a good agreement with the XRD analysis data demonstrating reduced sintering temperature (800 °C) necessary to produce cubic phase of YSZ. One can expect that the reduced thickness of the YSZ film will lower ohmic losses across the potential fuel cell where these layers could be applied as electrolyte [30, 31].

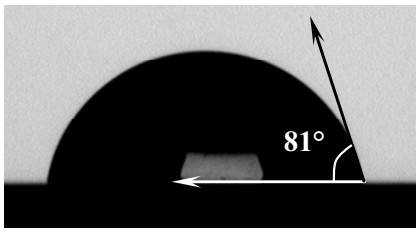

Fig. 7. Image of water droplet on the surface of YSZ coating obtained by the synthesis route (I)

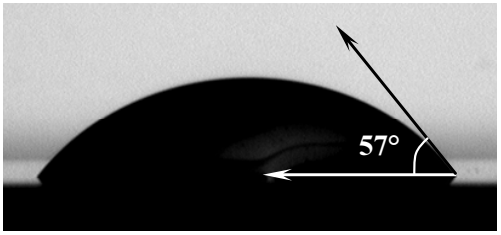

Fig. 8. Image of water droplet on the surface of YSZ coating obtained by the synthesis route (II)

In order to estimate hydrophobic properties of the produced thin films using different synthesis techniques the contact angle measurements (CAM) were performed. Roughness in both different synthesis routes is similar, but the hydrophobicity of YSZ films was found to be dependent on the used synthesis route. The contact angle

measurement results of 5 dipping and 5 annealing procedures formed by synthesis routes (I) and (II) are presented in Figs. 7 and 8.

As seen from Fig. 7, the contact angle of the alumina surfaces coated with YSZ layers using aqueous Y-Zr-O nitrate-tartrate sol is about 81°.

The highest spreading effect was observed for YSZ thin layers from yttrium and zirconium nitrate salts dissolved in 1.2-propanediol obtained by the synthesis route (II) (57°, Fig. 8).

4. CONCLUSIONS

New sol-gel methods for the preparation of nanostructured yttrium stabilized zirconia thin films on Al_2O_3 substrates using dip-coating technique have been developed. It was demonstrated that both an aqueous and non-aqueous sol-gel techniques are suitable for the formation of YSZ coatings. According to XRD analysis data both suggested synthesis routes are suitable for the preparation of thin submicronic YSZ films on Al_2O_3 substrate. The surface morphology of obtained YSZ thin films was almost identical independent on the used synthesis route. The hydrophobic properties of the produced thin films using different synthesis techniques were dependent on the used synthesis route and contact angle with distilled water varied between 81° and 57°.

Acknowledgments

This research was funded by a grant (No. ATE-05/2010) from the Research Council of Lithuania.

REFERENCES

1. **Will, J., Mitterdorfer, A., Kleinlogel, C., Perednis, D., Gauckler, L. J.** Fabrication of Thin Electrolytes for Second-generation Solid Oxide Fuel Cells *Solid State Ionics* 131 2000: pp. 79 – 96.
2. **Xu, X., Xia, C., Huang, S., Peng, D.** YSZ Thin Films Deposited by Spin-coating for IT-SOFCs *Ceramics International* 31 2005: pp. 1061 – 1064.
3. **Morales, M., Roa, J. J., Capdevila, X. G., Segarra, M., Pinol, S.** Mechanical Properties at the Nanometer Scale of GDC and YSZ Used as Electrolytes for Solid Oxide Fuel Cells *Acta Materialia* 58 2010: pp. 2504 – 2509.
4. **Zha, S., Zhang, Y., Liu, M.** Functionally Graded Cathodes Fabricated by Sol-gel/slurry Coating for Honeycomb SOFCs *Solid State Ionics* 176 2005: pp. 25 – 31.
5. **Liu, J., Barnett, S. A.** Thin Yttrium-stabilized Zirconia Electrolyte Solid Oxide Fuel Cells by Centrifugal Casting *Journal of American Ceramic Society* 85 2002: pp. 3096 – 3098.
6. **Viazzi, C., Bonino, J. P., Ansart, F., Barnabe, A.** Structural Study of Metastable Tetragonal YSZ Powders Produced via a Sol–gel Route *Journal of Alloys and Compounds* 452 2008: pp. 377 – 383.
7. **Diaz-Parralejo, A., Cuerda-Correa, E. M., Macias-Garcia, A., Diaz-Diez, M. A., Sanchez-Gonzalez, J.** Tailoring the Properties of Yttria-stabilized Zirconia Powders Prepared by the Sol-gel Method for Potential Use in Solid Oxide Fuel Cells, Fuel Processing Technology, doi:10.1016/j.fuproc.2010.05.033.
8. **Talebi, T., Raissi, B., Maghsoudipour, A.** The Role of Addition of Water to Non-aqueous Suspensions in Electrophoretically Deposited YSZ Films for SOFCs *International Journal of Hydrogen Energy* 35 2010: pp. 9434 – 9439.
9. **Cheng, J., Bao, W., Han, C., Cao, W.** A Novel Electrolyte for Intermediate Solid Oxide Fuel Cells *Journal of Power Sources* 195 2010: pp. 1849 – 1853.
10. **Gaudon, M., Laberty-Robert, C., Ansart, F., Stevens, P.** Thick YSZ Films Prepared via a Modified Sol-gel Route: Thickness Control (8–80 μm), *Journal of the European Ceramic Society* 26 2006: pp. 3153 – 3160.
11. **Ding, J., Liu, J.** An Anode-supported Solid Oxide Fuel Cell with Spray-coated Yttria-stabilized Zirconia (YSZ) Electrolyte Film *Solid State Ionics* 179 2008: pp. 1246 – 1249.
12. **Hu, L., Wang, C. A, Huang, Y., Sun, C., Lu, S., Hu, Z.** Control of Pore Channel Size during freeze Casting of Porous YSZ Ceramics with Unidirectionally Aligned Channels Using Different Freezing Temperatures *Journal of the European Ceramic Society* 30 2010: pp. 3389 – 3396.
13. **Tucker, M. C., Lau, G. Y., Jacobson, C. P., Visco, S. J., De Jonghe, L. C.** Cu-YSZ Cermet Solid Oxide Fuel Cell Anode Prepared by High-temperature Sintering *Journal of Power Sources* 195 2010: pp. 3119 – 3123.
14. **Ojha, P. K., Rath, S. K., Chongdar, T. K., Kulkarni, A. R.** Nanocrystalline Yttria Stabilized Zirconia by Metal-PVA Complexation *Ceramics International* 36 2010: pp. 561 – 566.
15. **Diaz-Parralejo, A., Ortiz, A. L., Rodriguez-Rojas, F., Guiberteau, F.** Effect of N_2 Sintering Atmosphere on the Hardness of Sol-gel Films of 3 mol% Y_2O_3-stabilized ZrO_2 *Thin Solid Films* 518 2010: pp. 2779 – 2782.
16. **Amezaga-Madrid, P., Antunez-Flores, W., Gonzalez-Hernandez, J., Saenz-Hernandez, J., Campos-Venegas, K., Solis-Canto, O., Ornelas-Gutierrez, C., Vega-Becerra, O., Martinez-Sanchez, R., Miki-Yoshida, M.** Microstructural Properties of Multi-nano-layered YSZ Thin Films *Journal of Alloys and Compounds* 495 2010: pp. 629 – 633.
17. **Brinker, C. J., Scherer, G. W.** Sol-Gel Science: The Physics and Chemistry of Sol-Gel Processing, Academic Press, London, 1990.
18. **Cushing, B. L., Kolesnichenko, V. L., O'Connor, C. J.** Recent Advances in the Liquid-phase Syntheses of Inorganic Nanoparticles *Chemical Reviews* 104 2004: pp. 3893 – 3946.
19. **Katelnikovas, A., Barkauskas, J., Ivanauskas, F., Beganskiene, A., Kareiva, A.** Aqueous Sol-gel Synthesis Route for the Preparation of YAG: Evaluation of Sol-gel Process by Mathematical Regression Model *Journal of Sol-gel Science and Technology* 41 2007: pp. 193 – 201.
20. **Mackenzie, J. D., Bescher, E. P.** Chemical Routes in the Synthesis of Nanomaterials Using the Sol-gel Process *Accounts of Chemical Research* 40 2007: pp. 810 – 818.
21. **Baranauskas, A., Jasaitis, D., Kareiva, A.** Characterization of Sol-gel Process in the Y-Ba-Cu-O acetate-tartrate System Using IR Spectroscopy *Vibrational Spectroscopy* 28 2002: pp. 263 – 275.
22. **Cizauskaite, S., Reichlova, V., Nenartaviciene, G., Beganskiene, A., Pinkas, J., Kareiva, A.** Sol-gel Preparation and Characterization of Gadolinium Aluminate *Materials Chemistry and Physics* 102 2007: pp. 105 – 110.

23. **Katelnikovas, A., Justel, T., Uhlich, D., Jorgensen, J.-E., Sakirzanovas, S., Kareiva, A.** Characterization of Cerium-Doped Yttrium Aluminium Garnet Nanopowders Synthesized via Sol-gel Process *Chemical Engineering Communications* 195 2008: pp. 758 – 769.
24. **Klemkiene, T., Raudonis, R., Beganskiene, A., Zalga, A., Grigoraviciute, I., Kareiva, A.** Scandium and Gallium Substitution Effects in the $(Y_{1-x}Sc_x)Ba_2Cu_4O_8$ and $(Y_{1-x}Ga_x)Ba_2Cu_4O_8$ Superconducting Oxides *Materials Chemistry and Physics* 119 2010: pp. 208 – 213.
25. **Barkauskas, J., Žaržojūtė, I., Kareiva, A.** Production and Contact Angle Measurements of Nano-structured Carbon Coatings *Chemija* 18 2007: pp. 12 – 16.
26. **Bogdanoviciene, I., Jankeviciute, A., Pinkas, J., Beganskiene, A., Kareiva, A.** Sol-gel Synthesis and Characterization of Kalsilite-type Alumosilicates *Materials Science* (*Medžiagotyra*) 13 2007: pp. 214 – 218.
27. **Philipavicius, J., Kazadojev, I., Beganskiene, A., Melninkaitis, A., Sirutkaitis, V., Kareiva, A.** Hydrophobic Antireflective Silica Coatings via Sol-gel Process *Materials Science* (*Medžiagotyra*) 14 2008: pp. 283 – 287.
28. **Skaudzius, R., Zalga, A., Kareiva, A.** Sol-gel Synthesis of Nanocrystalline $LaAlO_3$-M_2O_3 (M = La, Al) and Nd:$LaAlO_3$-M_2O_3 Composite Materials via „Phase Metathesis“ Route *Materials Science* (*Medžiagotyra*) 14 2008: pp. 193 – 197.
29. **Cizauskaite, S., Johnsen, S., Jørgensen, J.-E., Kareiva, A.** Sol-gel Preparation and Characterization of Non-substituted and Sr-substituted Gadolinium Cobaltates *Materials Chemistry and Physics* 125 2011: pp. 469 – 473.
30. **Beckel, D., Biebeerle-Hutter, A., Harvey, A., Infortuna, A., Muecke, U. P., Prestat, M., Rupp, J. L. M. Gauckler, L. J.** Thin Films for Micro Solid Oxide Fuel Cells *Journal of Power Sources* 173 2007: pp. 325 – 345.
31. **Egger, P., Soraru, G. D., Dire, S.** Sol-gel Synthesis of Polymer-YSZ Hybrid Materials for SOFC Technology *Journal of the European Ceramic Society* 24 2004: pp. 1371 – 1374.
32. **Viazzi, C., Deboni, A., Ferreira, J. Z., Bonino, J.-P., Ansart, F.** Synthesis of Yttria Stabilized Zirconia by Sol-gel Route: Influence of Experimental Parameters and Large Scale Production *Solid State Ionics* 8 2006: pp. 1023 – 1028.